CrystEngComm

Cite this: *CrystEngComm*, 2011, **13**, 3213

www.rsc.org/crystengcomm

PAPER

Heterosynthon mediated tailored synthesis of pharmaceutical complexes: a solid-state NMR approach†

Mujeeb Khan, Volker Enkelmann and Gunther Brunklaus*

Received 17th September 2010, Accepted 10th December 2010
DOI: 10.1039/c0ce00657b

Based on crystal engineering principles, we have explored the *predictability* of resulting structures of a multi-component pharmaceutical model complex derived from 4-hydroxybenzoic acid (4HBA) and quinidine, an anti-malarial constituent of *Cinchona* tree bark. Though the obtained complex is stabilized by a slightly different set of *charge-assisted heterosynthons* as proposed, the applied concept was efficient in predicting the salt formation. The salt **1** crystallizes in a monoclinic space group [$P2_1$ (no. 4), $Z = 8$, $a = 6.914$ Å, $b = 36.197$ Å, $c = 9.476$ Å and $\beta = 92.126$], where the asymmetric unit is comprised of two quinidine and two 4HBA molecules. In addition, a *micro-crystalline*, *less-defined* sample of **1** was obtained from rapid co-crystallization in *ethanol* and successfully identified *via* both infrared spectroscopy and multinuclear solid-state NMR. The interpretation of the obtained NMR data was supported by DFT quantum-chemical computations while illustrating options of "NMR crystallography".

1. Introduction

Most pharmaceuticals contain active pharmaceutical ingredients (APIs) in the form of molecular crystals and are frequently administered in the solid-state as part of an approved dosage type such as tablets or capsules.[1] Scientists constantly strive to improve physical properties of APIs, including *crystallinity*, stability, taste and (most importantly) *solubility*.[2] Indeed, drug molecules with limited aqueous *solubility* are rather challenging in pharmaceutical development and may pose the risk of insufficient or inconsistent exposure and thus poor efficacy in patients upon oral administration.[3] Therefore, the basic concepts of *crystal engineering*[4] have been recently utilized for tailored design of pharmaceuticals thereby providing a new path for (more) systematic discovery of a wider range of multi-component structures such as *pharmaceutical co-crystals*[5,6] and *salts* with properly adjusted pharmacokinetic and physical properties.[7] Both, *co-crystals* and *salts*, constitute multi-component compounds whose crystal structures are often dominated by the driving force of building a maximum of hydrogen bonds.[8] *Co-crystals*, however, comprise neutral molecules that are chemically distinct whereas *salts* are ionized and often *less*-ordered solids where a proton is typically transferred from an acid to a base.[9] Though many examples[10] of successful *co-crystallization*[11] are known, which yield solids with hydrogen bonding motifs expected from the principles of *crystal engineering*,[12] an exact prediction of resulting three-dimensional structures of solids obtained from such experiments is still a challenging task,[13,14] particularly in the case of less rigid fragments.[15]

Co-crystal formation in principle can be rationalized by consideration of hydrogen bond donors (D) and acceptors (A) present in the respective precursor materials. Though hydrogen bonds have been defined on the basis of interaction geometries found in crystal structures, certain effects in IR absorption spectra (*e.g.* red shift of ν_{DH}) or experimental electron density distributions, a necessary geometric criterion for reliable (rather strong) hydrogen bonding is a positive *directionality* preference, where "linear" D–H···A angles must be statistically favoured over bent ones.[16] Since a distribution of many D–H···A angles and even hydrogen bonds with more than one acceptor are feasible (*e.g.* "bifurcation"), a combination of multiple (even relatively weak) hydrogen bonds may lead to the formation of highly complex, rather stable molecular aggregates thereby indicating *cooperativity* of hydrogen bonding.[17] Ionic hydrogen bonds, however, constitute a particular class of interaction which is relevant for self-assembly of supramolecular moieties,[18] protein folding, many electrolytes and even ionic aggregates.[19] In particular, charge-assisted hydrogen bonds (CAHBs) consist of hydrogen bond acceptor and donor moieties where each of them carries an ionic charge that further reinforces the electrostatic dipole–dipole character of the hydrogen bond, thus rendering them preferably *linear* in geometry.[20] Notably, CAHBs in

Max-Planck-Institut für Polymerforschung, Postfach 31 48, D-55021 Mainz, Germany. E-mail: brunklaus@mpip-mainz.mpg.de

† Electronic supplementary information (ESI) available: Spectral data not figured in the manuscript such as simulated powder diffraction data, ^{1}H MAS and ^{1}H DQ MAS NMR spectra of the "*ethanol* phase" of salt **1**, a table of DFT computed chemical shifts, solid-state ^{15}N-CPMAS spectra of quinidine, *salt* **1**, infrared absorption spectra of 4HBA, quinidine, acetone and ethanol phases of *salt* **1**, the CIF file of salt **1** and complete ref. 83. CCDC reference number 804730. For ESI and crystallographic data in CIF or other electronic format see DOI: 10.1039/c0ce00657b

molecular crystals have been classified according to whether they are negative charge assisted (*e.g.*, $O^{-}\cdots H–O$), positive charge assisted (*e.g.*, $O\cdots H–N^{+}$), "neutral charge assisted" (*e.g.*, $O^{-}\cdots H–N^{+}$) or even resonance assisted (in this case two oxygens or nitrogens are connected by a system of π-conjugated double bonds).[21] Moreover, N–H donors with a formal positive charge tend to form shorter bonds than the corresponding uncharged N–H groups, while the negatively charged carboxylate ion is a stronger acceptor than uncharged amides, ketones or carboxyl moieties.[22]

Therefore, in the present work, while applying crystal engineering principles,[23] we explore the *predictability* of the resulting structures of a multi-component pharmaceutical model complex based on the robust and competitive $O–H\cdots N$[24] heterosynthon that may be comprised of either *neutral* ($O–H\cdots N$) or *charge-assisted* ($O^{-}\cdots H–N^{+}$) hydrogen bond mediated molecular recognition. In addition, the suitability of solid-state NMR for the structural characterization of *micro-crystalline* or rather *ill-defined* compounds that may be difficult to identify by other techniques is highlighted thereby illustrating options of NMR-based crystallography.[25] For this purpose, based on the compound classification Generally Recognized As Safe (GRAS),[26] we have selected *p*-hydroxybenzoic acid (4HBA) as the co-crystal former,[27] which is structurally highly related to established tablet excipients such as methyl paraben or gentisic acid, and therefore may also have the potential to be applied as an excipient. Though 4HBA has been previously used as a co-crystal former with tetramethylpyrazine (an important active ingredient of the Chinese herb *Ligusticum wallichii Franchat*),[28] any obtained formulations with 4HBA still have to be thoroughly evaluated for long term stability since pharmaceuticals are often prone to solid state reactions including phase transformations (*e.g.*, into different polymorphs), dehydration or desolvation as well as acid–base or transacylation reactions of the active pharmaceutical ingredients (APIs) and tablet excipients.[29]

4HBA provides both a hydroxyl group (OH) allowing for a neutral $O–H\cdots N$ heterosynthon and a carboxyl group (COOH) which is often known to engage in an ionized $O^{-}\cdots H–N^{+}$ heterosynthon with nitrogen bearing compounds such as pyridines or amines, provided that the ΔpK_a is sufficiently large (>3).[30] On the other hand we considered a representative API that possesses multiple accessible nitrogen atoms (preferably with different pK_a values) such as quinidine (*cf.* Scheme 1),[24] an anti-malarial constituent of Cinchona tree bark which can be used as *anti*-arrythmatic agent with *anti*-muscarinic and alpha-adrenoceptor blocking properties[31] or for treatment of neurological disorders.[32]

Equimolar co-crystallization of 4HBA with quinidine from *acetone* has yielded a crystalline *molecular salt* **1** that is stabilized *via* charge-assisted $O^{-}\cdots H–N^{+}$ units, whereas co-crystallization from *ethanol* produced an apparently *ill-defined* compound which was identified as *micro-crystalline salt* **1** by both infrared spectroscopy and solid-state NMR. While infrared spectroscopy is typically applied to monitor changes of the sample identity with respect to a given reference compound including the detection of either counterfeit medicines[33] or successful co-crystal formation (particularly when carboxylic acids are involved),[2a] modern high-resolution solid-state NMR (at high magnetic fields and rather fast magic-angle spinning) constitutes a powerful tool

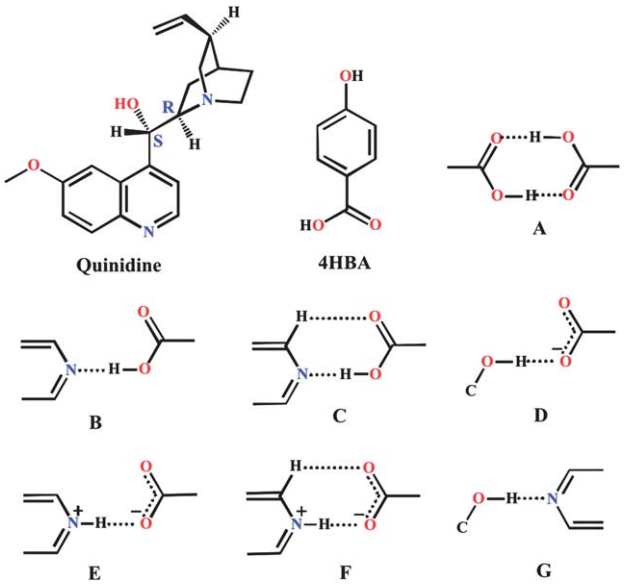

Scheme 1 Chemical structures and supramolecular homo- and heterosynthons offered by pure quinidine, *p*-hydroxybenzoic acid (4HBA) and *molecular salt* **1**. (a) acid dimer, (b) acid–pyridine single point neutral, (c) acid-pyridine two point neutral, (d) acid–phenol single point ionic, (e) acid–pyridine single point ionic, (f) acid–pyridine two point ionic and (g) phenol–pyridine single point neutral.

that allows for detailed structural characterization of powdered materials,[34] including pharmaceutical co-crystals[24] and complexes,[35] even in the absence of X-ray structural data.

Notably, NMR not only affords non-invasive, element specific observation of different nuclei thereby providing outstanding selectivity for local environments,[36] but also facilitates an identification of chemically distinct sites based on NMR chemical shifts.[37] In particular, protons involved in hydrogen-bonded structures exhibit well-resolved ^{1}H chemical shifts mainly between 8 and 20 ppm (depending on their geometry),[38] rendering an estimation of hydrogen-bonding strengths feasible,[39] as *e.g.* documented by established empirical correlations between ^{1}H isotropic chemical shifts and corresponding hydrogen bonding strengths, *i.e.* specified by $O\cdots H$, $N\cdots H$ or $O\cdots O$ distances, respectively, by X-ray analysis,[40] neutron[41] and even electron diffraction.[42] Additional structural insights may be obtained from double-quantum ^{1}H MAS NMR where homonuclear $^{1}H–^{1}H$ dipolar couplings correlate protons of different chemical entities thereby providing both precise information on proton–proton proximities as well as distances[43] (which in principle can be very fruitful for unambiguous identification of *pharmaceutical salts*) on length scales of up to 3.5 Å[44] and proton positions in arrays of multiple hydrogen bonds.[45] Moreover, the combination of solid-state NMR spectroscopy with density functional theory (DFT)[46] computations not only corroborates chemical shift assignments but in some cases also provides an approach to "*NMR crystallography*",[47] which allowed for both polymorph screening,[48] *e.g.* in hydrochloride pharmaceuticals,[49] and even powder structure determination of small drug molecules[50] or precursors for synthesis of graphite-like carbon nitrides, respectively.[51] Nevertheless, *de novo* NMR-based structure solutions without or only minor support from

additional X-ray data of functional compounds are still rather scarce. In many cases, however, merely *local* complex formation is of prime interest, which is indeed immediately accessible *via* solid-state NMR.

2. Results and discussion

Based on extensive statistical studies of the Cambridge Structural Database[52] (CSD) addressing selected hydrogen-bonding motifs,[30] it has been reported that a variety of supramolecular *hetero*synthons are fairly reliable for successful preparation of co-crystals and often formed preferentially compared to *homo*-synthons.[14] In particular, the strong and rather specific recognition among either carboxylic acids and pyridine(s) (COOH···N)[53] or phenols and pyridine(s) (O–H···N)[14] has been well studied. Indeed, many *co-crystals* have been obtained based on carboxylic acid and heterocyclic-N hydrogen-bonding,[5,53] including the abundantly used co-crystal former isonicotinamide (a member of the vitamin B group),[54] in addition to *molecular salts* (*i.e.*, the proton is transferred from the acid to base).[9] In contrast, the interaction of phenolic hydroxyl groups (OH) with pyridine almost exclusively has produced *co-crystals*.[14,36b]

Notably, four variants of the acid–pyridine heterosynthon are found in the corresponding crystal structures: (i) neutral, two point; (ii) neutral, single point; (iii) ionic, two point; and (iv) ionic, single point (Scheme 1).[27] The acid–pyridine neutral two point synthon (*cf.* Scheme 1c) occurrence probability is around 90% when other competing functional groups are absent. However, when there is a sufficient pK_a (ΔpK_a = [pK_a base] − [pK_a acid] > 3) difference between the COOH and pyridyl group, a *proton transfer* will occur resulting in the formation of ionic hydrogen bonds ($O^-\cdots H–N^+$ (*cf.* Scheme 1e and f)), thus yielding *molecular salts*.[9]

Therefore, 4HBA and quinidine have been selected as model compounds to form a *multi*component molecular complex that *may* be stabilized by both neutral (O···H–N) or charge assisted ($O^-\cdots H–N^+$) heterosynthons. Quinidine consists of three basic molecular units, a quinoline aromatic ring, a quinuclidine ring (a tertiary amine), and a methylenic alcohol group linking the two (*cf.* Scheme 1). In its pure form, quinidine crystallizes in a monoclinic space group ($P2_1$ (no. 4); $Z = 2$; $a = 11.883$ Å, $b = 7.037$ Å, $c = 11.256$ Å), with the unit cell comprised of two quinidine molecules that are stabilized by intermolecular hydrogen-bonding among the C11-hydroxyl group and the N-atom of the quinuclidine ring while the N-atom of the quinoline ring remains free.[24] According to *crystal engineering* principles, nitrogen atoms of both quinuclidine and quinoline rings with pK_a values of 8.4 and 4.25 respectively[55] and the carboxyl (COOH) and hydroxyl (OH) groups of 4HBA with pK_a value of 4.48 constitute possible targets for hydrogen-bond mediated molecular recognition of both *neutral* and *charge assisted* heterosynthons (*cf.* Scheme 2).

In our previous work, *co-crystal* formation of quinidine and methyl paraben based on the *neutral* O–H···N heterosynthon has been successfully demonstrated,[24] where the quinuclidine nitrogen was hydrogen-bonded to a hydroxyl group (OH) of methyl paraben. However, when methyl paraben is replaced by 4HBA, we expected that the COOH group (best donor)[28] of 4HBA could be hydrogen-bonded to the same nitrogen thereby

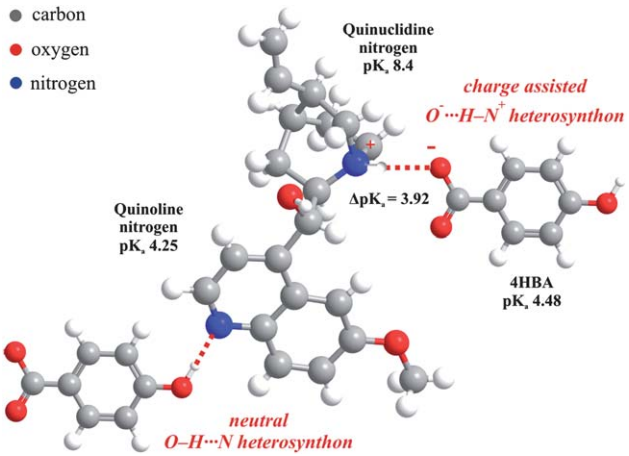

Scheme 2 proposed model for the synthesis of multi-component pharmaceutical complex comprised of both charge assisted ($O^-\cdots H–N^+$) and neutral (O–H···N) hydrogen-bond mediated molecular recognition of heterosynthons based on *crystal engineering* principles.

forming a charge assisted $O^-\cdots H–N^+$ heterosynthon, mainly owing to the pK_a difference of more than 3 between the quinuclidine N atom and 4HBA, respectively. In addition, the hydroxyl group (OH, second best donor) of 4HBA should be engaged in a neutral O–H···N heterosynthon with the quinoline N atom of quinidine, thus leading to a chain like structure (*cf.* Scheme 2). Though considerable efforts have been made to explicitly define synthons[4] and their use in supramolecular synthesis of pharmaceutical complexes,[24] the predictions of the result of such preparation is still not reliable.[13,14] Nevertheless, there have been some rather promising attempts to predict the resulting crystal structures of 1 : 1 molecular co-crystals and solvates using a chemical diagram[56] or more recently, computed crystal energy landscapes,[57] including the co-crystal structure of caffeine with 4HBA.[58] Yet, the solid form resulting from experiments targeting molecular complexes comprised of *ionic* synthons (such as *molecular salts*) may be even more challenging to predict due to the tendency of *charge assisted* complexes to have alternating lattice compositions.[9a] This is nicely demonstrated based on a survey of 85 solids (either *salts* or *co-crystals*) obtained from stoichiometric mixtures of a carboxylic acid with an N-heterocyclic base, where it was found that 45% of the "salt structures" were either solvates or had a different stoichiometric composition than implied from the expected hydrogen bonding in contrast to only 5% in the case of the co-crystals.[9a]

Equimolar co-crystallization of quinidine and 4HBA in *acetone* has yielded the *salt* **1** (Fig. 1) rather than the anticipated molecular complex shown in Scheme 2. It crystallizes in a monoclinic space group [$P2_1$ (no. 4), $Z = 8$, $a = 6.914$ Å, $b = 36.197$ Å, $c = 9.476$ Å and $\beta = 92.126$] with significantly larger *b*-axis, where the asymmetric unit comprises two quinidine and two 4HBA molecules respectively. Indeed, the quinuclidinic N-atom in **1** is part of a charge assisted single point $O^-\cdots H–N^+$ heterosynthon, where the proton is transferred from the carboxyl group of 4HBA to the N-atom of the quinuclidine ring, just as predicted. However, the N-atom of the quinoline ring did not get involved in any type of hydrogen-bonding and remained "*free*" in **1**, similarly to pure quinidine. Hence, *no neutral* O–H···N

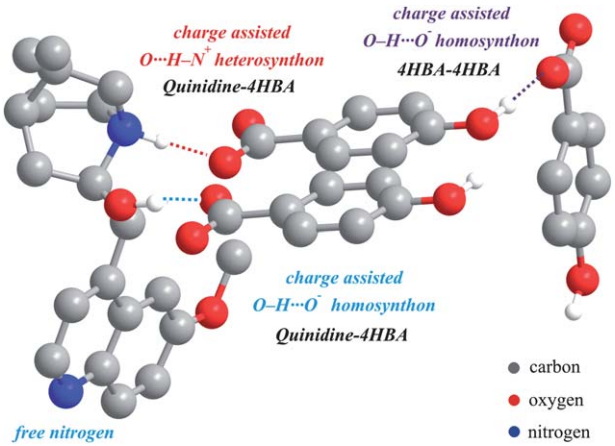

Fig. 1 Portion of the molecular packing of pharmaceutical *salt* **1** obtained from quinidine and 4HBA depicting the total number of hydrogen bonds responsible for stabilizing the structure. All hydrogen atoms are omitted for clarity except for those involved in hydrogen bonding (dotted lines represent the hydrogen bond).

heterosynthon[24] is formed between the OH group of 4HBA and the N-atom of the quinoline ring in **1**. Rather, the hydroxyl group (OH) of 4HBA is hydrogen-bonded to the carboxylate group (COO^-) of an another 4HBA molecule within the asymmetric unit of **1** reflecting a charge assisted O–H···O^- homosynthon (Scheme 1d). Notably, the crystal structure of pristine 4HBA comprises the *commonly found* hydrogen bonding motif of a carboxylic acid dimer (Scheme 1a),[59] while there is no direct hydrogen-bonding between the 4-hydroxyl (OH) and carboxylic acid groups. Clearly, such COOH dimer formation among 4HBA molecules is absent in **1**. Rather, one of the oxygen atoms in the carboxylate group of 4HBA acts as hydrogen-bond acceptor for hydroxyl groups (OH) of both quinidine and 4HBA (*cf.* Fig. 1). In summary, the crystal structure of **1** is stabilized by three types of *charge assisted* synthons, one ionic single point O^-···H–N^+ heterosynthon and two O–H···O^- homosynthons, while interestingly, upon co-crystallization of 4HBA with pyridine, a neutral compound can be obtained.[60]

Though selective hydrogen-bonding constitutes the preferred interaction in crystal engineering studies,[61] which is known to significantly contribute to physical properties or reactivity[36b] of molecular complexes or supramolecular aggregates,[62] its characterization by X-ray analysis is difficult. In most cases, hydrogen atoms are calculated with standard distances into a refined structure of heteroatoms and are practically left unrefined.[63] Therefore, characteristic distances between donor–acceptor pairs (such as N···O, O···O) are more reliable and thus quite useful to distinguish the formation of either a *salt* or "neutral" *co-crystal*. Other important factors in known structures of *co-crystals* and *salts*, such as different C–O bond lengths in carboxylate and carboxylic acid,[36a] as well as sensitivity of the C–N–C angle of pyridine to protonation at its nitrogen atom may also serve to determine the nature of a compound. Notably, the average ratio of C–O (long) to C–O (short) bond lengths is ~1.027 for *salts* and ~1.081 for *co-crystals*. Corresponding C–N–C angles on neutral pyridine-based molecules are reported to be in the range of 117.7–118.5°, while protonated analogues can have bond angles over 120°.[9a]

Indeed, the refined single crystal X-ray structure of the 1 : 1 complex of quinidine and 4HBA indicates successful formation of a *salt*: the measured C–O bond distances of the carboxylate group (COO^-) of 4HBA in **1** are 1.261 Å and 1.231 Å with an average ratio of 1.024, which is very close to the reported ratio of *salts*.[9a] Moreover, the measured C–N–C angles of the aliphatic quinuclidine ring in **1** (109.63°, 109.17° and 112.26°) are slightly larger than the corresponding C–N–C angles of the quinuclidine ring in the "neutral" 1 : 1 *co-crystal* of quinidine and methylparaben (107.97°, 107.23°, 111.13°),[24] in good agreement with the expected trend in the case of *salt* formation.

As stated earlier, equimolar co-crystallization of both quinidine and 4HBA from *acetone* yielded colorless *well-defined* prism-shaped *crystals* of **1** while a similar attempt of rapid co-crystallization from *ethanol* produced a rather *glassy* substance sticking to the wall of the container, which turned into a white sticky powder upon scratching. Since the physical states of both samples were quite different we acquired the respective powder X-ray diffraction patterns (Fig. 2) to possibly identify other phases or impurities. Notably, the diffractogram of the "*acetone* phase" with its *sharp* and *well*-resolved peaks clearly indicated a *crystalline* nature of the sample. The pattern is almost identical to a simulated powder pattern of **1** (*cf.* ESI†), whereas the large "bump" with *smaller* and *blurred* (highly *un*resolved) peaks in the powder pattern of the "*ethanol* phase" point towards a reduced *bulk crystallinity* of the sample (*e.g.*, *ill*-defined or rather *micro*-crystalline). Nevertheless, at this point, it is not clear whether the compound from *ethanol* reflects the molecular *salt* **1** or another *polymorph*.

Upon close inspection of the respective powder diffractograms of both samples (*crystalline* and apparently *ill*-defined), the rather weak diffraction peaks on top of the large bump ("*ethanol* phase") clearly *coincide* with the more prominent peaks of the "*acetone* phase" hence indicating a very similar molecular packing (Fig. 2). Since the identity of a considered pharmaceutical formulation (and in some cases even the amount of an active ingredient within a tablet) can be established *via* infrared (IR) spectroscopy,[64] we recorded the corresponding IR absorption spectra of quinidine, 4HBA as well as both the *acetone* and *ethanol* phases of *salt* **1** (ESI†), which indeed exhibit a number of distinct differences in the fingerprint and high frequency region. While this clearly indicates changes in the nature of the respective sample, IR spectroscopy may be used as a primary method only if artificial calibration samples with the same composition and structure as the samples to be analyzed are available. Nevertheless, the absence of a strong C=O stretching band around 1700 cm^{-1} in the "*acetone* phase" hints at formation of carboxylate (COO^-) anions,[65] and the observable high energy shift of the OH stretching band from around 3380 cm^{-1} in the case of 4HBA to 3422 cm^{-1} in *salt* **1** may reflect changes of the hydrogen bonding pattern upon complex formation. Apart from these features, however, the IR absorption spectrum of **1** is highly unresolved (*e.g.* due to strong peak overlapping of both 4HBA and quinidine resonances) rendering structural assignments and identification of the formed complex rather difficult.

In contrast, solid-state NMR provides outstanding selectivity for local environments, even in the case of *ill-defined*, *powdered* compounds, often facilitating unambiguous identification of chemically distinct sites based on the corresponding NMR

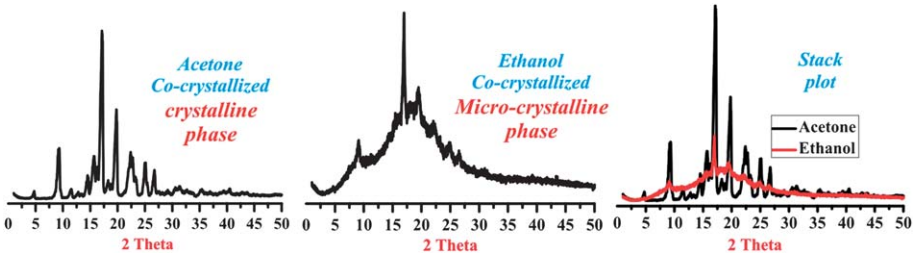

Fig. 2 Powder X-ray diffraction pattern of the compounds obtained from co-crystallization of quinidine and 4HBA using either *acetone* or *ethanol* reflecting the *well*-defined *crystalline* and apparently *ill*-defined nature of the samples.

chemical shifts (even in the absence of X-ray data).[25,40] In particular, the sensitivity of ^{13}C (or ^{15}N) chemical shifts to small changes in the local environment can be considered as a fingerprint to rather quickly identify whether co-crystallization has produced an intact *co-crystal* (or *salt*) or eventually a random mixture of *co-crystal* formers, which in the case of simpler mixtures may be also feasible *via* IR spectroscopy.[33] In the absence of X-ray data, an NMR-based structure determination would at first require identification of the asymmetric unit, which in principle can be deduced from the corresponding ^{13}C-CPMAS spectra (Fig. 3), provided that sufficient spectral resolution can be achieved. Notably, for molecular compounds with low space group symmetry, the integrant unit (which is the first multiple of the asymmetric unit leading to integer number of atoms reflecting the stoichiometry of the considered crystal formula) is often equivalent to the molecule comprising the crystal.

In the case of **1**, well-resolved peaks reflecting individual signals, *i.e.*, due to either quinidine or 4HBA, were found, thereby tentatively suggesting that the asymmetric unit may be comprised of one quinidine and one 4HBA molecule, though the asymmetric unit of **1** as derived from X-ray analysis contains *two* quinidine and *two* 4HBA molecules, respectively. Their local environments, however, are rather similar so that merely one set of ^{13}C peaks is observed for both quinidine and 4HBA. Similarly, this applies to pristine quinidine, thus illustrating that for molecular crystals, sometimes integer multiples of the initially guessed number of molecules comprising the asymmetric have to be considered. The carbon signals of 4HBA in **1** experienced significant shifts compared to those of the pure form, where in particular, C49 and C50 shifted from 171.7 to 174.2 ppm and 123.3 to 132.5 ppm, respectively, indicating both different hydrogen-bonding environments and changes in the *ionization*

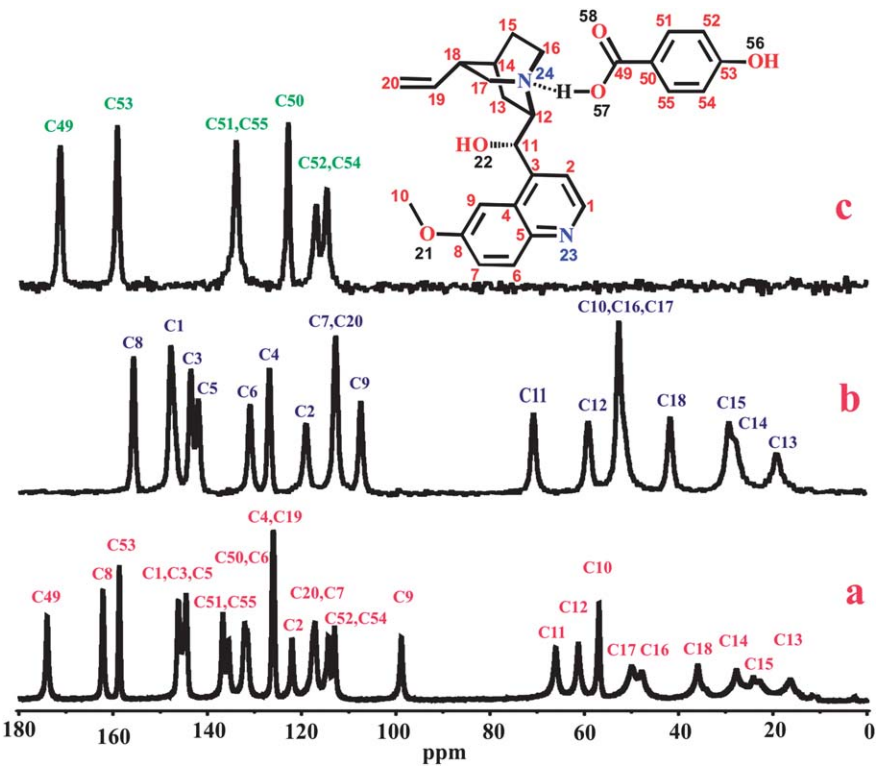

Fig. 3 Solid-state ^{13}C-CPMAS spectra of (a) *salt* **1**, (b) quinidine,[24] and (c) *p*-hydroxybenzoic acid (4HBA). All ^{13}C-CPMAS spectra were collected at 75.5 MHz using a Bruker Avance-II 300 machine with contact time of 2 ms, co-adding 8196 transients. The experiments were carried out using a standard 4 mm double-resonance MAS probe spinning at 12 kHz, typical $\pi/2$ pulse length of 4 μs, and a recycle delay of 5 s. All spectra were acquired at room temperature, while the given peak assignments are based on DFT computations (see ESI†).

state of the carboxylic acid group of 4HBA (*i.e.*, formation of the carboxylate ion due to proton transfer from 4HBA to quinidine)[35a] upon complex formation, in good agreement with the IR data. In pure 4HBA,[27,28] the carboxyl group is engaged in a dynamic hydrogen-bonding[36a] typically found for an acid dimer (Scheme 1a) while in **1** such interaction is clearly absent. Rather, the proton of the carboxyl group has been transferred from 4HBA to the quinuclidine nitrogen (N24) resulting in *salt* formation. Moreover the hydroxyl group of 4HBA (which is engaged in a hydrogen-bonded charge assisted O–H···O$^-$ homosynthon with the carboxyl group of another 4HBA molecule in **1**) is not involved in any kind of hydrogen bonding in its pure form. Most ^{13}C signals of quinidine within **1** displayed minor changes of 1–2 ppm owing to a slightly different molecular packing, except the signals of C7 (shifted from 113.8 to 118.0 ppm) and C9 (shifted from 107.8 to 99.3 ppm) of the quinoline ring that have shifted ≈7 ppm (Fig. 3), reflecting the changed conformation of the methoxy group (C10) in **1**.[24] In addition, significant shifts of 4–5 ppm were also observed for some aliphatic carbons of the quinuclidine ring possibly owing to conformational changes of its C=C group.

The ^{13}C chemical shift assignment (Fig. 3) is given based on DFT computations (at B3LYP/6-311 + G** level of theory)[36] of an optimized cutout from the crystal structure of **1** that includes representative hydrogen bonding environments (where all non-hydrogen atoms were frozen on their crystallographic positions) while ignoring packing effects.[66] In particular, we applied the recently introduced multi-standard (MSD) approach[67] which is sufficiently accurate (particularly for molecular systems) but computationally less demanding than highly electron-correlated approaches[68] or even full consideration of crystal lattice effects.[69]

After confirming that the compound obtained from co-crystallization of quinidine and 4HBA in *acetone* is *salt* **1** ("*acetone* phase"), an unambiguous identification of the *micro*crystalline compound ("*ethanol* phase") was considered. Clearly, the corresponding IR spectra of both phases (ESI†) are indistinguishable hence indicating an *identical* nature of the two compounds even though the powder diffractogram of the "*ethanol* phase" was highly unresolved (*unlike* the *well*-defined "*acetone* phase").

Likewise, its ^{13}C-CPMAS spectrum exhibited *sharp* and *well*-defined peaks, yet with slightly broader lines than the "*acetone* phase" (Fig. 4), where the presence of small "bumps" at the shoulder of some signals may be caused by more *disordered* fractions of the sample. This clearly demonstrates that solid-state NMR (and to some extent IR spectroscopy) can be efficiently applied to characterize even those *micro*-crystalline pharmaceutical *co-crystals* or *salt* that cannot be (unambiguously) identified using X-ray powder diffraction analysis.[70]

Furthermore, ^{1}H MAS NMR spectra were recorded in order to in detail analyze the local hydrogen bonding environments and characteristic signatures of the salt identity of both compounds, which is particularly beneficial in view of NMR-based structure determination of related compounds in the possible absence of X-ray data. Similarly to the IR and ^{13}C-CPMAS spectra, both phases revealed almost identical ^{1}H MAS NMR spectra including observable linewidths (ESI†). The peak at 12.06 ppm in the corresponding ^{1}H MAS NMR spectrum of **1** (Fig. 5) is clearly indicative of a different hydrogen-bonding pattern in **1** compared to both pristine 4HBA or quinidine and

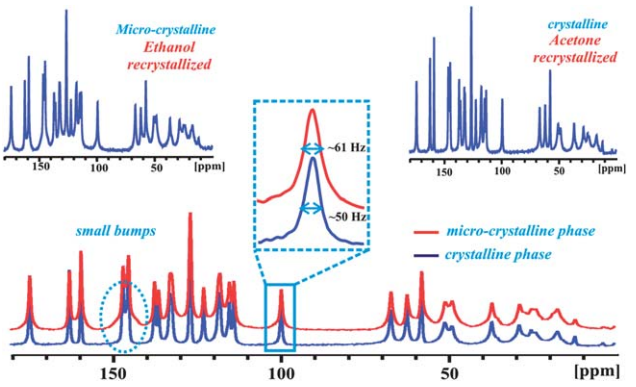

Fig. 4 ^{13}C-CPMAS spectra of both *well*-defined *crystalline* ("*acetone* phase") and rather *micro-crystalline* ("*ethanol* phase") compounds obtained from co-crystallization of quinidine and 4HBA in either *acetone* or *ethanol*. Note the slightly increased linewidth and the presence of smaller "bumps" at the shoulder of some signals in the ^{13}C-CPMAS spectrum of the "*ethanol* phase".

even the previously reported co-crystal of quinidine and methyl paraben.[24] While it is obvious that a dimer formation of carboxylic acid units in **1** can be excluded, the ^{1}H signal at 12.06 ppm cannot be readily assigned. The distance of heavy atoms within the charge assisted O$^-$···H–N$^+$ heterosynthon in the salt **1** (d(N–O) = 2.661 Å) is only slightly larger than the corresponding distance within the neutral O···H–N heterosynthon (d(N–O) = 2.620 Å) of the quinidine/methyl paraben co-crystal,[24] but in the latter case, the NH proton resonates at 13.45 ppm. Notably, all hydrogen-bonds considered here fall within the range of "classical" moderately strong hydrogen-bonds,[62] where the distance of the heavy atoms is less than the sum of their van-der-Waals radii (N···O 3.22 Å, O···O 3.04 Å).[71] While moderate "stretching" of the distance between heavy atoms embracing a hydrogen-bonded proton typically leads to reduced ^{1}H chemical shifts (*i.e.*, indicating weaker bonds),[40,72] the introduction of positive charges often result in strongly increased ^{1}H chemical shifts, and hence the opposite.[45b] Within the neutral O···H–N heterosynthon of pristine quinidine, a heavy atom distance of d(N–O) = 2.760 Å and an NH proton peak at 9.34 ppm were observed. Since the convenient case of rather linear hydrogen bonding is considered, we may be tempted to also assume a linear dependence of the ^{1}H chemical shift of the NH proton with respect to d(N–O), at least in the given range of 2.62 to 2.76 Å, although commonly, a fixed heavy atom distance is applied where the proton approaches the respective hydrogen-bond acceptor.[37] Nevertheless, considering Δd(N–O) = 0.14 Å and $\Delta\delta$ = 4.01 ppm (yielding an apparent increment of ≈0.286 ppm per 0.01 Å, ignoring charge effects), we can "predict" the ^{1}H chemical shift of O$^-$···H–N$^+$ in **1** at 12.16 ± 0.2 ppm, which on one hand is remarkably close to the experimental value of 12.06 ppm but on the other hand could be purely fortuitous.

Though the additional ^{1}H MAS NMR signals at 8.3 ppm and 8.78 ppm may be tentatively assigned to the protons within charge assisted O–H···O$^-$ homosynthons formed between the hydroxyl groups of both quinidine and 4HBA with a carboxylate group of 4HBA, possible peak overlap with resonances from aromatic protons cannot be excluded. However, a DFT ^{1}H chemical shift computation (at B3LYP/6-311 + G** level of

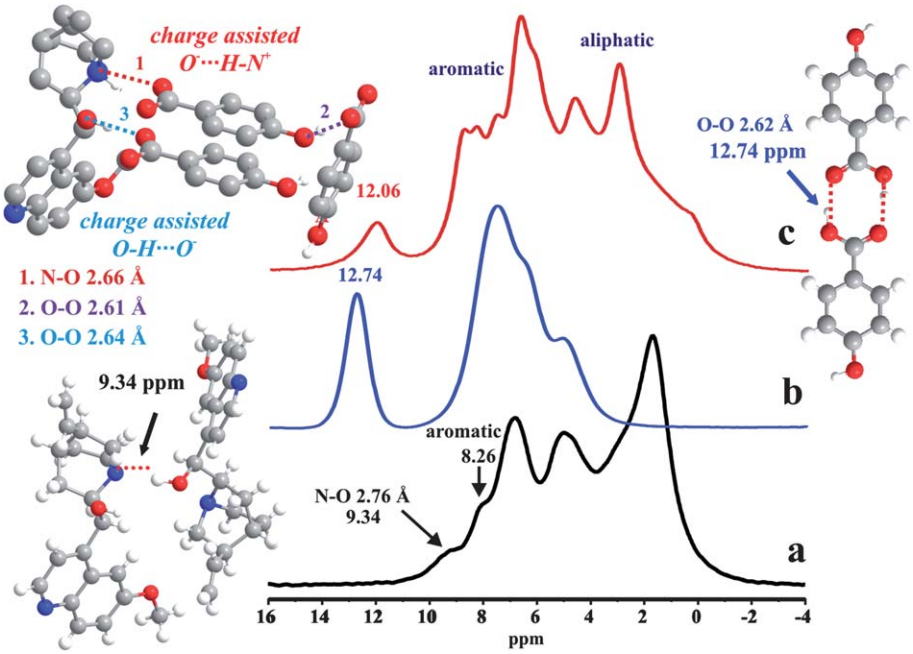

Fig. 5 ^{1}H MAS NMR spectra of (a) quinidine, (b) 4-hydroxybenzoic acid (4HBA), and (c) *salt* **1**, acquired at 850.1 MHz using a commercially available Bruker 2.5 mm double resonance MAS probe at a spinning frequency of 29762 Hz, typical $\pi/2$ pulse lengths of 2 μs, and a recycle delay of 5–10 s, co-adding 32 transients.

theory)[36] based on an optimized model cutout from the crystal structure of **1** predicts ^{1}H chemical shifts of 12.9 ppm ($O^{-}\cdots H$–N^{+}), 11 ppm (O–H$\cdots O^{-}$, quinidine–OH, COO^{-} of 4HBA) and 11.6 ppm (O–H$\cdots O^{-}$, 4HBA–OH, COO^{-} of another 4HBA), respectively, with ±1.5 ppm for each value, rendering all hydrogen-bonded protons barely distinguishable. Aromatic protons were computed at 7–9 ppm, in reasonable agreement with the experimental data.

^{1}H–^{1}H double-quantum (DQ) NMR is in general a highly useful and selective approach to identify close contacts or spatial proximities of structural moieties and can be used to reveal changes of hydrogen-bonding environments, *i.e.* upon successful formation of pharmaceutical co-compounds or salts. In such a two-dimensional experiment, double-quantum coherences (DQC) due to *pairs* of dipolar coupled protons are correlated with single-quantum coherences resulting in characteristic correlation peaks. Double-quantum coherences between so-called *like* spins appear as a single correlation peak on the diagonal ("auto-peak") while a pair of cross-peaks that are symmetrically arranged on either side of the diagonal reflect couplings among *unlike* spins. DQ peaks appear at the sum frequency of the two coupled spins and therefore often allow for an increased spectral resolution.

In addition, we exploit the fact that observable double-quantum signal intensities are proportional to D_{ij}^{2} or r_{ij}^{-6}, respectively (D_{ij} is the homonuclear dipolar coupling constant, r_{ij} the internuclear distance), at least in the limit of short dipolar recoupling times (*i.e.*, 16.8–33.6 μs). Strong signal intensities in the corresponding double-quantum spectrum therefore reveal protons in rather close spatial proximity (*i.e.* distances up to 3.5 Å).[73] In contrast, rather weak DQ signals reflect either long-distance contacts or the presence of fast local molecular dynamics (with respect to the timescale of the experiment). Hence, in order to provide further evidence of co-compound formation and peak assignments of the corresponding ^{1}H MAS NMR spectrum of **1**, fast MAS ^{1}H DQ spectra of both the crystalline "*acetone* phase" and micro-crystalline "*ethanol* phase" (*cf.* ESI†) of *salt* **1** were recorded at two different recoupling times ($T_R/2$ = 16.8 μs and T_R = 33.6 μs, respectively) (Fig. 6). According to the hydrogen-optimized model cutout of the crystal structure, the shortest distance of the NH^{+} proton to both aromatic and aliphatic protons amounts to d = 2.216 Å (D_{ij} = 11.04 kHz) and d = 2.366 Å (D_{ij} = 9.07 kHz), respectively, while the quinidine–OH proton has a comparable proximity to aromatic protons (d = 2.206 Å, D_{ij} = 11.19 kHz) but a longer distance to aliphatic protons (d = 2.658 Å, D_{ij} = 6.41 kHz). In contrast, the 4HBA–OH proton is close to two different aromatic protons (d = 2.204 Å, D_{ij} = 11.22 kHz; d = 2.279 Å, D_{ij} = 10.15 kHz) but further away from aliphatic protons (d = 2.904 Å, D_{ij} = 4.91 kHz). Since the dipolar couplings among the protons are very sensitive with respect to the distance (*cf.* static dipolar couplings D_{ij} given in brackets), this should indeed be reflected by the observed DQ signal intensities. In particular, the presence of the DQ peak at 15.36 ppm (12.06 ppm + 3.3 ppm) strongly suggests that the ^{1}H peak at 12.06 ppm reflects the NH^{+} proton which is involved in *salt* formation (*i.e.*, the proton is transferred from the carboxyl group of 4HBA to the quinuclidine nitrogen (N24) of quinidine), as the signal at ~3.3 ppm (in good agreement with the DFT ^{1}H chemical shift computation) represents aliphatic protons of the quinuclidine ring of quinidine. This is further supported by a rather strong cross-peak at 18.76 ppm (12.06 ppm + 6.67 ppm) reflecting the contact of the NH^{+} proton with its closest CH moiety (the bridging C*H*OH). In contrast, the cross-peak at 20.51 ppm (11.74 ppm + 8.77 ppm) indicates the

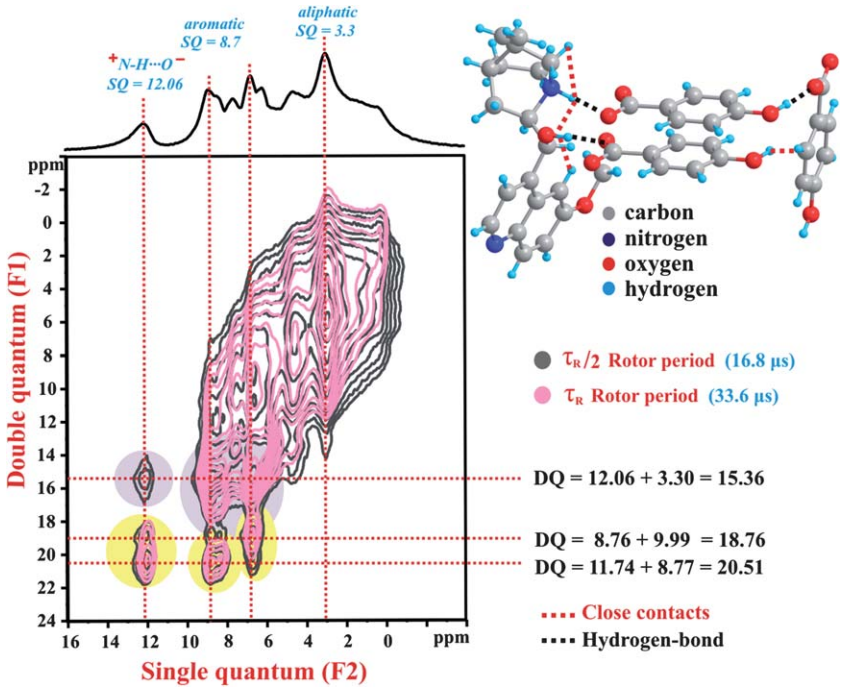

Fig. 6 ^{1}H–^{1}H DQ MAS NMR spectrum of the *salt* **1** at 850.1 MHz and 29762 Hz MAS, acquired under the following experimental conditions: $\tau_{(exc.)}$ = 16.8 μs (or 33.6 μs), 64 t_1 increments at steps of 33.6 μs, relaxation delay 60 s, 16 transients per increment. Sixteen positive contour levels between 10% and 100% (or 15% and 100%) of the maximum peak intensity were plotted. The *F2* projection is shown on the top; the most important DQ cross-peaks are highlighted.

presence of an additional hydrogen-bonded proton site whose resonance in the regular ^{1}H MAS NMR spectrum most likely is buried under the fairly broad (full width at half height ≈1.1 ppm) but slightly asymmetric peak centered at 12.06 ppm. Based on the ^{1}H chemical shift computation, this site is assigned to the 4HBA–OH protons (computed at 11.6 ppm), whose closest aromatic protons are computed at 8.9 ppm. Two further moderately strong cross-peaks present in the ^{1}H DQ MAS spectrum of **1** applying the shortest possible dipolar recoupling time of $T_R/2$ (in our case 16.8 μs) at 18.76 ppm (8.77 ppm + 9.99 ppm) and (8.35 ppm + 10.41 ppm), however, cannot be unambiguously assigned. While at first glance it may appear feasible to attribute the "obtained" peaks at either 9.99 ppm or 10.41 ppm to the quinidine–OH proton (computed at 11 ppm), such resonances cannot be identified in the corresponding ^{1}H MAS NMR spectrum of **1**. Therefore, those signals possibly reflect multi-spin effects such as "DQ relay" where an initially formed DQ coherence couples with at least a third spin yielding apparent DQ peaks (*i.e.*, at the sum of three chemical shifts). This, however, requires sufficiently strong dipolar couplings among the spins and a suitable geometry (hence spatial proximity), which in principle could be exploited for NMR-based structure determination, but is rarely applied to organic samples. Nevertheless, multi-spin effects could be further probed by ^{1}H triple-quantum MAS NMR,[74] which is beyond the scope of this work.

In favourable cases, particularly in the case of dipolar coupled clusters (*i.e.*, triple- or quadruple hydrogen-bonded moieties), selected internuclear proton–proton distances (derived from ^{1}H–^{1}H dipolar couplings) may be quantitatively determined if either so-called DQ spinning sideband pattern[75] or DQ signal build-up curves[76] are generated. Since the corresponding ^{1}H DQ MAS spectra of both the "*acetone* phase" and "*ethanol* phase" of **1** are virtually identical while corroborating the presence of NH^+ (hence indicating salt formation), we refrained from a full determination of the hydrogen substructures of the charge-assisted synthons. Nevertheless, the hydrogen bonding parameters obtained from the partially optimized representative cutout from the crystal structure for the corresponding synthons $O^-\cdots H–N^+$ (d(N···O) = 2.661 Å, d(N–H) = 1.067 Å, <(NHO) = 161.2°), O–H···O^- (4HBA–OH, COO^- of another 4HBA; d(O···O) = 2.618 Å, d(O–H) = 0.989 Å, <(OHO) = 173.0°) and O–H···O^- (quinidine–OH, COO^- of 4HBA; d(O···O) = 2.642 Å, d(O–H) = 1.005 Å, <(OHO) = 169.7°) are fairly similar to previously reported data of binary co-crystals and salts,[53b] indicating that the respective proton within the O–H···O^- synthons is involved in almost ideally linear hydrogen bonding (bond angle ≈170 to 180°).

Further insight into the structural environment of both crystalline "*acetone* phase" and micro-crystalline "*ethanol* phase" of **1** was obtained from ^{15}N CPMAS NMR. The ^{15}N chemical shift is rather sensitive to packing or coordination effects and benefits from a larger chemical shift range and pronounced anisotropic properties thereby providing superior resolution, particularly in cases where nitrogen atoms are partially protonated. Indeed, a reliable interpretation of such data requires comparison with similar known compounds or quantum-chemical shift computations of model structures.[77] In the case of **1**, *two* resonances at −74.2 ppm and −337.0 ppm with rather narrow linewidths about 60 Hz were observed in the 1D ^{15}N CPMAS spectrum

(ESI†), indicating a high degree of crystallinity[42] and magnetic equivalence of the two quinidine molecules contained in the asymmetric unit of **1**, whereas the corresponding ^{15}N CPMAS spectrum of pure quinidine displays signals at −73.6 ppm and −344.0 ppm. Notably, the minor shift of 0.6 ppm of the signal at 74.2 ppm in **1** (assigned to the quinoline ring)[24] with respect to pure quinidine clearly reveals that the nitrogen atom (N23) of the quinoline ring in **1** does *not* engage in hydrogen bonding, similarly to its pure form. In contrast, the remaining signal at −337.0 ppm (assigned to N24 atom of quinuclidine ring in **1**)[24] is shifted ∼7 ppm to higher ppm compared to the chemical shift of N24 (−344.0 ppm) in pure quinidine. Notably, the computed ^{15}N chemical shifts of −66.8 ppm (N23) and −343.4 ppm (N24), respectively, are in reasonable agreement with the experimentally observed values (within ±7.5 ppm), particularly the marginal upfield shift upon co-crystallization. This in turn implies that the DFT optimized hydrogen-bonding environment taken from the crystal structure is rather representative. Similar to the ^{1}H and ^{13}C NMR spectra, the ^{15}N CPMAS spectra of the *crystalline* ("*acetone* phase") and *micro-crystalline* ("*ethanol* phase") compound obtained from co-crystallization of quinidine and 4HBA are rather comparable except for slightly increased linewidths (about 70 Hz rather than 60 Hz) in the latter case.

According to a recent report,[78] for a heterocyclic and fairly basic nitrogen, an upfield shift (*i.e.*, larger negative ppm values) of about 20 up to 40 ppm has been observed in the case of strong hydrogen-bonding, while upfield shifts of even 80 ppm or more may occur if a proton is transferred from a donor (such as carboxylic acid) to an acceptor nitrogen. Notably, similar trends were also observed in the reported co-crystal of quinidine and methylparaben,[24] *i.e.*, a marginal upfield shift (∼2.5 ppm) was found when replacing a moderate hydrogen bond to a comparatively strong hydrogen bond. However, in the case of **1**, the quinuclidine nitrogen (N24) is rather protonated, as revealed by its single crystal and NMR analysis. This finding may be attributed to two facts: at one hand the presumed upfield shift of ∼80 ppm[49] may be preferably observed in cases where a previously *free* nitrogen atom is protonated. The quinuclidinic nitrogen (N24), however, was not *free* even in its pure form (N24 is hydrogen-bonded to the hydroxyl group of another quinidine molecule and exhibits an ^{15}N chemical shift of −344 ppm). On the other hand, observable upfield shifts tend to increase upon contraction of the corresponding N–O distances, thus yielding stronger hydrogen bonds in neutral compounds (*co-crystals*), while the opposite trend is found for charged species (*salts*).[49] Since the N–O distance in the case of pure quinidine amounts to 2.76 Å, which shrinks to 2.66 Å upon co-crystallization with 4HBA, the shift of ∼7 ppm to higher ppm could well be explained.

3. Conclusion

In this work, we have explored the predictability of resulting structures of a multi-component pharmaceutical model complex based on 4-hydroxybenzoic acid (4HBA) and quinidine, an anti-malarial constituent of *Cinchona* tree bark. Though the *salt* is stabilized by a slightly different set of heterosynthons as proposed based on crystal engineering principles, the concept was almost efficient in predicting the *salt* formation. The obtained *salt* crystallizes in a monoclinic space group [$P2_1$ (no. 4), $Z = 8$, $a = 6.914$ Å, $b = 36.197$ Å, $c = 9.476$ Å and $\beta = 92.126$] with significantly larger *b*-axis, where the asymmetric unit is comprised of two quinidine and two 4HBA molecules. In addition, a *micro-crystalline*, *less-defined* sample of *salt* **1** was obtained from rapid co-crystallization in *ethanol*, and successfully identified *via* IR spectroscopy and multinuclear solid-state NMR. The results were discussed with respect to "*NMR-based crystallography*" of structurally *less-defined* co-compounds, where an interpretation of the obtained NMR data was supported by DFT quantum-chemical computations, thereby illustrating the great potential of solid-state NMR for complementary application in the fast screening and structural analysis of pharmaceutical complexes[79] (including co-crystals and salts) obtained under similar conditions (*i.e.*, fast evaporation).

4. Experimental section

Both quinidine ((9*S*)-6′-methoxycinchonan-9-ol and *p*-hydroxybenzoic acid (4HBA) were purchased from Aldrich and used as obtained. Pharmaceutical salt of 4HBA and quinidine were prepared by dissolving 1 mmol of quinidine (324.4 mg) and 1 mmol of 4HBA (138.12 mg) in 50 ml acetone. The solution was left for slow evaporation in an open container (50 ml crystallizing dish). After two days, colourless *well-defined* prism-like crystals were obtained and subsequently ground to powder for structural characterization *via* powder X-ray diffraction and solid-state NMR. In order to obtain sufficiently large crystals suitable for single crystal X-ray analysis, the same solution was left for slow evaporation in a test tube. However, when *ethanol* was used under similar conditions except fast evaporation (within 1–2 days) of the solution in a crystallizing dish, colourless *glassy* substance sticking to the wall of the dish was obtained. Upon scratching a white, *ill-defined* rather micro-crystalline powder (as identified by powder X-ray diffraction) could be retrieved which was later identified as *salt* **1** *via* solid-state NMR. Nevertheless, when the same solution of quinidine and 4HBA (in ethanol) was left for much *slower* evaporation over a period of 2–3 weeks in an open glass tube, then *well-defined* white micro-crystalline powder (confirmed by powder X-ray diffraction data) similar to the one obtained by acetone were formed. However, the quality of those crystals was not good enough to be analyzed by single crystal X-ray diffraction.

Solid-state NMR methods

Proton solid-state NMR data were recorded at 850.1 MHz employing a Bruker Avance III spectrometer, while ^{13}C-CPMAS spectra were recorded at 75.5 MHz using a Bruker Avance-II 300 machine. Most experiments were carried out using a commercially available Bruker 2.5 mm double-resonance MAS probe at a spinning frequency of 29762 Hz, typical π/2-pulse lengths of 2 μs and recycle delays of 5–10 s. The spectra were referenced with respect to tetramethylsilane (TMS) using solid adamantane as the secondary standard (1.63 ppm for ^{1}H and 29.456 ppm for ^{13}C). In addition, ^{15}N-CPMAS spectra were recorded at 30.4 MHz using a Bruker Avance-II 300 machine and referenced to

solid $^{15}NH_4Cl$ (−341.0 ppm). If not stated otherwise, all spectra were collected at room temperature. The back-to-back (BaBa)[80] recoupling sequence was used to excite and reconvert double-quantum coherences, applying States-TPPI[81] for phase sensitive detection. Further details are given in the figure captions of the respective 2D-spectra.

DFT-based chemical shift calculations

The proton positions of a selected fragment of the crystal structure reflecting representative hydrogen-bonding environments were optimized with all heavy atoms fixed at the crystallographic positions *via* DFT quantum chemical calculations, applying the B3LYP functional and 6-311G[82] split valence basis set augmented with diffuse and polarization functions. Subsequently, ^{1}H, ^{13}C and ^{15}N chemical shifts with respect to either tetramethylsilane (TMS, ^{1}H), benzene (^{13}C) and methanol (^{13}C) or nitromethane (^{15}N) were computed at B3LYP/6-311 + G** level of theory with the GIAO approach as implemented in the Gaussian03 program.[83] Note that the recently introduced multi-standard approach is applied in the case of ^{13}C.[67]

Single crystal structure analysis

Crystal parameters of **1** are reported as follows: colourless prism-like crystals, which were crystallized in a monoclinic space group [$P2_1$ (no. 4), $Z = 8$, $a = 6.914$ Å, $b = 36.197$ Å, $c = 9.476$ Å and $\beta = 92.126$]. Data collection at 120 K was done on a Nonius KCCD diffractometer ($Mo_{K\alpha}$ ($\lambda = 0.71073$ Å)), equipped with a graphite monochromator. The intensity data were corrected for Lorentz and polarization effects, while structure solution and refinement were performed employing the SHELXS86[84] and CRYSTALS[85] software packages. All *non*-hydrogen atoms were refined in the anisotropic approximation against F of all observed reflections. The hydrogen atoms were refined in the riding mode with fixed isotropic temperature factors; **1**: R-factor (%) = 3.74.

Infrared spectroscopy

Infrared absorption spectra were obtained at a resolution of 4 cm^{-1} using a Perkin Elmer FTIR BXII model Fourier transform infrared spectrometer using potassium bromide pellets of the compounds.

Acknowledgements

Financial support from the Deutsche Forschungsgemeinschaft (DFG) through the SFB 625 in Mainz is gratefully acknowledged.

References

1 S. Dutta and D. J. W. Grant, *Nat. Rev. Drug Discovery*, 2004, **3**, 42–47.
2 (*a*) N. Schultheiss and A. Newman, *Cryst. Growth Des.*, 2009, **9**, 2950–2967; (*b*) S. Byrn, R. Pfeiffer, M. Ganey, C. Hoiberg and G. Poochikian, *Pharm. Res.*, 1995, **12**, 945–954; (*c*) Z. Ma and B. Moulton, *J. Chem. Crystallogr.*, 2009, **39**, 913–918.
3 (*a*) N. Blagden, M. De Metas, P. T. Gavan and P. York, *Adv. Drug Delivery Rev.*, 2007, **59**, 617–630; (*b*) L. F. Huang and W. Q. Tong, *Adv. Drug Delivery Rev.*, 2004, **56**, 321–324.
4 (*a*) G. R. Desiraju, *Angew. Chem., Int. Ed.*, 2007, **46**, 8342–8356; (*b*) G. R. Desiraju, *Angew. Chem., Int. Ed. Engl.*, 1995, **34**, 2311–2327; (*c*) G. R. Desiraju, *Nat. Mater.*, 2002, **1**, 77–79; (*d*) G. R. Desiraju, *Nature*, 2001, **412**, 397–400.
5 (*a*) S. L. Childs, L. J. Chyall, J. T. Dunlap, V. N. Smolenskaya, B. C. Stahly and G. P. Stahly, *J. Am. Chem. Soc.*, 2004, **126**, 13335–13342; (*b*) J. F. Remenar, S. L. Morissette, M. L. Peterson, B. Moulton, J. M. MacPhee, H. R. Guzman and O. Almarsson, *J. Am. Chem. Soc.*, 2003, **125**, 8456–8457; (*c*) L. S. Reddy, N. B. Jagadeesh and A. Nangia, *Chem. Commun.*, 2006, 1369–1371.
6 (*a*) S. L. Childs and M. J. Zaworotko, *Cryst. Growth Des.*, 2009, **9**, 4208–4211; (*b*) N. Shan and M. J. Zaworotko, *Drug Discovery Today*, 2008, **13**, 440–446; (*c*) D. R. Weyna, T. Shattock, P. Vishweshwar and M. J. Zaworotko, *Cryst. Growth Des.*, 2009, **9**, 1106–1123; (*d*) J. A. Bis, P. Vishweshwar, D. Weyna and M. J. Zaworotko, *Mol. Pharmaceutics*, 2007, **4**, 401–416.
7 (*a*) S. H. Jeong, Y. Takaishi, Y. Fu and K. Park, *J. Mater. Chem.*, 2008, **18**, 3527–3535; (*b*) S. L. Morissette, O. Almarsson, M. L. Peterson, J. F. Remenar, M. J. Read, A. V. Lemmo, S. Ellis, M. J. Cima and C. R. Gardner, *Adv. Drug Delivery Rev.*, 2004, **56**, 275–300; (*c*) A. V. Trask, *Mol. Pharmaceutics*, 2007, **4**, 301–309.
8 (*a*) C. B. Aakeröy and K. R. Seddon, *Chem. Soc. Rev.*, 1993, **22**, 397–407; (*b*) J. Bernstein, M. C. Etter and L. Leiserowitz, *Struct. Correl.*, 1994, **2**, 431–507; (*c*) K. Biradha, *CrystEngComm*, 2003, **5**, 374–384; (*d*) C. B. Aakeröy, J. Desper and M. E. Fasulo, *CrystEngComm*, 2006, **8**, 586–588.
9 (*a*) C. B. Aakeröy, M. E. Fasulo and J. Desper, *Mol. Pharmaceutics*, 2007, **4**, 317–322; (*b*) S. L. Childs, G. P. Stahly and A. Park, *Mol. Pharmaceutics*, 2007, **4**, 323–338.
10 (*a*) C. B. Aakeröy, A. M. Beatty and B. A. Helfrich, *Angew. Chem., Int. Ed.*, 2001, **40**, 3240–3242; (*b*) C. B. Aakeröy and D. J. Salamon, *CrystEngComm*, 2005, **7**, 439–448.
11 (*a*) M. Khan, V. Enkelmann and G. Brunklaus, *CrystEngComm*, 2009, **11**, 1001–1005; (*b*) L. R. MacGillivary, J. L. Reid and J. A. Ripmeester, *J. Am. Chem. Soc.*, 2000, **122**, 7817–7818.
12 (*a*) O. Almarsson and M. J. Zaworotko, *Chem. Commun.*, 2004, 1889–1896; (*b*) S. L. Childs, L. J. Chyall, J. T. Dunlap, V. N. Smolenskaya, B. C. Stahly and G. P. Stahly, *J. Am. Chem. Soc.*, 2004, **126**, 13335–13342.
13 P. G. Karamertzanis, A. V. Kazantsev, I. Nizar, G. W. A. Welch, C. S. Adjiman, C. C. Pantelides and S. L. Price, *J. Chem. Theory Comput.*, 2009, **5**, 1432–1448.
14 M. Khan, V. Enkelmann and G. Brunklaus, *Cryst. Growth Des.*, 2009, **9**, 2354–2362.
15 K. Chow, H. H. Y. Tong, S. Lum and A. H. L. Chow, *J. Pharm. Sci.*, 2008, **97**, 2855–2877.
16 T. Steiner and G. R. Desiraju, *Chem. Commun.*, 1998, 891–892.
17 I. Rozas, *Phys. Chem. Chem. Phys.*, 2007, **9**, 2782–2790.
18 J. M. Lehn, *Supramolecular Chemistry: Concepts and Perspectives*, Wiley, 1995.
19 M. Meot-Ner, *Chem. Rev.*, 2005, **105**, 213–284.
20 M. D. Ward, *Struct. Bonding*, 2009, **132**, 1–23.
21 (*a*) P. Gilli, V. Bertolasi, V. Ferretti and G. Gilli, *J. Am. Chem. Soc.*, 1994, **116**, 909–915; (*b*) S. J. Grabowski, *Annu. Rep. Prog. Chem., Sect. C*, 2006, **102**, 131–165.
22 R. Taylor and O. Kennard, *Acc. Chem. Res.*, 1984, **17**, 320–326.
23 C. B. Aakeröy and N. Schultheiss, in *Making Crystals by Design*, Wiley-VCH, Weinheim, 2007, pp. 209–240.
24 M. Khan, V. Enkelmann and G. Brunklaus, *J. Am. Chem. Soc.*, 2010, **132**, 5254–5263.
25 *NMR Crystallography*, ed. R. K. Harris, R. Wasylishen and M. Duer, Wiley, Chichester, 2009.
26 *The GRAS list*, http://www.fda.gov/Food/FoodIngredientsPackaging/GenerallyRecognizedasSafeGRAS/default.htm.
27 B. Sarma, N. K. Nath, B. R. Bhogala and A. Nangia, *Cryst. Growth Des.*, 2009, **9**, 1546–1557.
28 B. R. Sreekanth, P. Vishweshwar and K. Vyas, *Chem. Commun.*, 2007, 2375–2377.
29 S. R. Byrn, W. Xu and A. W. Newman, *Adv. Drug Delivery Rev.*, 2001, **48**, 115–136.
30 T. R. Shattock, K. D. Arora, P. Vishweshwar and M. J. Zaworotko, *Cryst. Growth Des.*, 2008, **8**, 4533–4545.
31 (*a*) A. M. Wahbi, M. S. Moneed, I. I. Hewala and M. F. Bahnasy, *Chem. Pharm. Bull.*, 2008, **56**, 787–879; (*b*) S. Kashino and

M. Haisa, *Acta Crystallogr., Sect. C: Cryst. Struct. Commun.*, 1983, **39**, 310–312; (*c*) B. Pniewska and A. Suszko-Purzycka, *Acta Crystallogr., Sect. C: Cryst. Struct. Commun.*, 1989, **45**, 638–642.
32 R. A. Smith, *Expert Opin. Pharmacother.*, 2006, **7**, 2581–2591.
33 (*a*) A. C. Moffat, S. Assi and R. A. Watt, *J. Near Infrared Spectrosc.*, 2010, **18**, 1–15; (*b*) A. J. O'Neill, R. D. Jee, G. Lee, A. Charvill and A. Moffat, *J. Near Infrared Spectrosc.*, 2008, **16**, 327–333.
34 (*a*) D. Reichert, *Annu. Rep. NMR Spectrosc.*, 2005, **55**, 159–203; (*b*) S. E. Ashbrook and M. E. Smith, *Chem. Soc. Rev.*, 2006, **35**, 718–735; (*c*) S. P. Brown, *Prog. Nucl. Magn. Reson. Spectrosc.*, 2007, **50**, 199–251.
35 (*a*) F. G. Vogt, J. S. Clawson, M. Strohmeier, A. J. Edwards, T. N. Pham and S. A. Watson, *Cryst. Growth Des.*, 2009, **9**, 921–937; (*b*) F. G. Vogt, J. A. Vena, M. Chavda, J. S. Clawson, M. Strohmeier and M. E. Barnett, *J. Mol. Struct.*, 2009, **932**, 16–30.
36 (*a*) M. Khan, G. Brunklaus, V. Enkelmann and H. W. Spiess, *J. Am. Chem. Soc.*, 2008, **130**, 1741–1748; (*b*) M. Khan, V. Enkelmann and G. Brunklaus, *J. Org. Chem.*, 2009, **74**, 2261–2270; (*c*) A. M. Orendt and J. C. Facelli, *Annu. Rep. NMR Spectrosc.*, 2007, **62**, 115–178.
37 R. K. Harris, *Solid State Sci.*, 2004, **6**, 1025–1037.
38 H. Szatylowicz, *J. Phys. Org. Chem.*, 2008, **21**, 897–914.
39 (*a*) H. H. Limbach, in *Hydrogen Transfer Reactions*, ed. J. T. Hynes, J. P. Klinman, H. H. Limbach and R. L. Schowen, Wiley-VCH, 2007; (*b*) S. P. Brown and H. W. Spiess, *Chem. Rev.*, 2001, **101**, 4125–4155; (*c*) R. Gobetto, C. Nervi, E. Valfrè, M. R. Chierotti, D. Braga, L. Maini, F. Grepioni, R. K. Harris and P. Y. Ghi, *Chem. Mater.*, 2005, **17**, 1457–1466.
40 (*a*) R. K. Harris, in *Encyclopedia of Nuclear Magnetic Resonance*, Wiley, Chichester, 1996, vol. 5, p. 3314; (*b*) R. K. Harris, Y. Phuong, B. Robert, C. Y. Ma and K. J. Roberts, *Chem. Commun.*, 2003, 2834–2835.
41 T. Emmler, S. Gieschler, H. H. Limbach and G. Buntkowsky, *J. Mol. Struct.*, 2004, **700**, 29–38.
42 T. Gorelik, G. Matveeva, U. Kolb, T. Schleuß, A. F. M. Kilbinger, J. van de Streek, A. Bohle and G. Brunklaus, *CrystEngComm*, 2010, **12**, 1824–1832.
43 J. P. Bradley, C. Tripon, C. Filip and S. P. Brown, *Phys. Chem. Chem. Phys.*, 2009, **11**, 6941–6952.
44 M. Schulz-Dobrick, T. Metzroth, H. W. Spiess, J. Gauss and I. Schnell, *ChemPhysChem*, 2005, **6**, 315–327.
45 (*a*) I. Schnell, B. Langer, S. H. M. Söntjens, R. P. Sijbesma, M. H. P. van Genderen and H. W. Spiess, *Phys. Chem. Chem. Phys.*, 2002, **4**, 3750–3758; (*b*) I. Bolz, C. Moon, V. Enkelmann, G. Brunklaus and S. Spange, *J. Org. Chem.*, 2008, **73**, 4783–4793.
46 (*a*) P. Geerlings, F. De Proft and W. Langenaeker, *Chem. Rev.*, 2003, **103**, 1793–1873; (*b*) R. G. Parr and W. Yang, *Density Functional Theory of Atoms and Molecules*, Oxford University Press, Oxford, 1989.
47 (*a*) B. Elena, G. Pintacuda, N. Mifsud and L. Emsley, *J. Am. Chem. Soc.*, 2006, **128**, 9555–9560; (*b*) C. J. Pickard, E. Salager, G. Pintacuda, B. Elena and L. Emsley, *J. Am. Chem. Soc.*, 2007, **129**, 8932–8933; (*c*) F. Taulelle, *Solid State Sci.*, 2004, **6**, 1053–1057; (*d*) J. Senker, L. Seyfarth and J. Voll, *Solid State Sci.*, 2004, **6**, 1039–1052.
48 (*a*) R. K. Harris, *J. Pharm. Pharmacol.*, 2007, **59**, 225–239; (*b*) R. K. Harris, *Analyst*, 2006, **131**, 351–373; (*c*) J. Thun, L. Seyfarth, J. Senker, R. E. Dinnebier and J. Breu, *Angew. Chem., Int. Ed.*, 2007, **46**, 6729–6731.
49 H. Hamaed, J. M. Pawlowski, B. F. T. Cooper, R. Fu, S. H. Eichhorn and R. W. Schurko, *J. Am. Chem. Soc.*, 2008, **130**, 11056–11065.
50 E. Salanger, R. S. Stein, C. J. Pickard, B. Elena and L. Emsley, *Phys. Chem. Chem. Phys.*, 2009, **11**, 2610–2621.
51 L. Seyfarth, J. Sehnert, N. E. A. El-Gamel, W. Milius, E. Kroke, J. Breu and J. Senker, *J. Mol. Struct.*, 2008, **889**, 217–228.
52 F. H. Allen, *Acta Crystallogr., Sect. B: Struct. Sci.*, 2002, **58**, 380–388.
53 (*a*) M. Sharmarke, D. A. Tocher, M. Vickers, P. G. Karamertzains and S. L. Price, *Cryst. Growth Des.*, 2009, **9**, 2881–2889; (*b*) C. B. Aakeröy, I. Hussain, S. Forbes and J. Desper, *CrystEngComm*, 2007, **9**, 46–54.
54 (*a*) C. B. Aakeröy, A. M. Beatty and B. A. Helfrich, *Cryst. Growth Des.*, 2003, **3**, 159–165; (*b*) A. Lemmerer, N. B. Báthori and S. A. Bourne, *Acta Crystallogr., Sect. B: Struct. Sci.*, 2008, **64**, 780–790; (*c*) P. Vishweshwar, A. Nangia and V. M. Lynch, *Cryst. Growth Des.*, 2003, **3**, 783–790.
55 D. C. Warhurst, J. C. Craig, I. S. Adagul, D. J. Meyer and S. Y. Lee, *Malar. J.*, 2003, **2**, 1–14.
56 (*a*) A. J. C. Cabeza, G. M. Day and W. Jones, *Chem.–Eur. J.*, 2008, **14**, 8830–8836; (*b*) A. J. C. Cabezy, G. M. Day, W. D. S. Motherwell and W. Jones, *J. Am. Chem. Soc.*, 2006, **128**, 14466–14467.
57 S. L. Price, *Acc. Chem. Res.*, 2009, **42**, 117–126.
58 M. Habgood and S. L. Price, *Cryst. Growth Des.*, 2010, **10**, 3263–3272.
59 B. M. Kariuki, C. L. Bauer, K. D. M. Harris and S. J. Teat, *Angew. Chem., Int. Ed.*, 2000, **39**, 4485–4488.
60 L. H. Wei, *Acta Crystallogr., Sect. E: Struct. Rep. Online*, 2006, **62**, 4506–4507.
61 (*a*) R. A. Weatherhead-Kloster, H. D. Selby, W. B. Miller, III and E. A. Mash, *J. Org. Chem.*, 2005, **70**, 8693–8702; (*b*) K. K. Arora and V. R. Pedireddi, *J. Org. Chem.*, 2003, **68**, 9177–9185; (*c*) L. R. MacGillivray, *J. Org. Chem.*, 2008, **73**, 3311–3317.
62 N. Tosa, A. Bende, R. A. Varga, A. Terec, I. Bratu and I. Grosu, *J. Org. Chem.*, 2009, **74**, 3944–3947.
63 T. Steiner, *Angew. Chem., Int. Ed.*, 2002, **41**, 48–76.
64 E. Bouveresse, C. Casolino and C. de la Pezuela, *J. Pharm. Biomed. Anal.*, 1998, **18**, 35–42.
65 (*a*) H. G. Brittain, *Cryst. Growth Des.*, 2009, **9**, 3497–3503; (*b*) C. B. Aakeröy, D. J. Salmon, M. M. Smith and J. Desper, *Cryst. Growth Des.*, 2006, **6**, 1033–1042.
66 (*a*) P. Lazzeretti, *Prog. Nucl. Magn. Reson. Spectrosc.*, 2000, **36**, 1–88; (*b*) J. A. N. F. Gomes and R. B. Mallion, *Chem. Rev.*, 2001, **101**, 1349.
67 A. M. Sarotti and S. C. Pellegrinet, *J. Org. Chem.*, 2009, **74**, 7254–7260.
68 J. Gauss and J. F. Stanton, *Adv. Chem. Phys.*, 2002, **123**, 355–422.
69 D. Stueber, *Concepts Magn. Reson., Part A*, 2006, **A28**, 347–368.
70 K. D. M. Harris and E. Y. Cheung, *Chem. Soc. Rev.*, 2004, **33**, 526–538.
71 P. A. Frey, *Magn. Reson. Chem.*, 2001, **39**, S190–S198.
72 M. R. Chierotti and R. Gobetto, *Chem. Commun.*, 2008, 1621–1634.
73 J. P. Bradley, C. Tripon, C. Filip and S. P. Brown, *Phys. Chem. Chem. Phys.*, 2009, **11**, 6941–6952.
74 I. Schnell, A. Lupulescu, S. Hafner, D. E. Demco and H. W. Spiess, *J. Magn. Reson.*, 1998, **133**, 61–69.
75 G. P. Holland, B. R. Cherry and T. M. Alam, *J. Magn. Reson.*, 2004, **167**, 161–167.
76 L. Seyfarth and J. Senker, *Phys. Chem. Chem. Phys.*, 2009, **11**, 3522–3531.
77 P. Lorente, I. G. Shenderovich, N. S. Golubev, G. S. Denisov, G. Buntkowsky and H. H. Limbach, *Magn. Reson. Chem.*, 2001, **39**, 18–29.
78 Z. J. Li, Y. Abramov, J. Bordner, J. Leonard, A. Medek and A. V. Trask, *J. Am. Chem. Soc.*, 2006, **128**, 8199–8210.
79 C. A. Lepre, J. M. Moore and J. W. Peng, *Chem. Rev.*, 2004, **104**, 3641–3675.
80 (*a*) J. Geen, J. Titman, J. Gottwald and H. W. Spiess, *Chem. Phys. Lett.*, 1994, **227**, 79–86; (*b*) J. Gottwald, D. E. Demco, R. Graf and H. W. Spiess, *Chem. Phys. Lett.*, 1995, **243**, 314–323; (*c*) K. Saalwächter, R. Graf and H. W. Spiess, *J. Magn. Reson.*, 2001, **148**, 398–418.
81 D. Marion, M. Ikura, R. Tschudin and A. Bax, *J. Magn. Reson.*, 1989, **85**, 393–399.
82 R. Krishnan, J. S. Binkley, R. Seger and J. A. Pople, *J. Chem. Phys.*, 1980, **72**, 650–654.
83 M. J. Frisch, et al., *Gaussian 03 (Revision D.02)*, Gaussian, Inc., Wallingford, CT, 2004.
84 G. M. Sheldrick, *SHELXS-86, Program Package for Crystal Structure Solution and Refinement*, Univeristät Göttingen, Germany, 1986.
85 P. W. Betteridge, J. R. Carruthers, R. I. Cooper, K. Prout and D. J. Watkin, *J. Appl. Crystallogr.*, 2003, **36**, 1487–1487.